

# A Realization of the Haldane-Kane-Mele Model in a System of Localized Spins

Se Kwon Kim, Héctor Ochoa, Ricardo Zarzuela, and Yaroslav Tserkovnyak

*Department of Physics and Astronomy, University of California, Los Angeles, California 90095, USA*

(Dated: December 3, 2024)

We theoretically study a spin Hamiltonian for spin-orbit-coupled ferromagnets on the honeycomb lattice. We find that the effective Hamiltonian for magnons, a quanta of spin-wave excitations from ordered states, is equivalent to the Haldane model for electrons in the honeycomb lattice, which indicates the nontrivial topology of the magnon bands and the existence of the associated edge state. We also take the Schwinger boson (or bosonic spinon) representations of spins that are applicable both to ordered and disordered phases. We show that the spinon bands within the mean-field treatment are topologically nontrivial, which causes a spin Nernst effect, by adopting the properties of the Kane-Mele model. A feasible experimental realization of the spin Hamiltonian is proposed.

PACS numbers: 85.75.-d, 75.47.-m, 73.43.-f, 72.20.-i

*Introduction.*— Electronic systems with spin-orbit coupling (SOC) can exhibit spin Hall effects, in which a longitudinal electrical field generates a transverse spin current and vice versa [1]. In particular, Kane and Mele [2] showed that a single plane of graphene has a topologically nontrivial band structure with an SOC-induced energy gap, which gives rise to a quantum spin Hall effect characterized by a quantized spin Hall conductivity. This identification of graphene as a quantum spin Hall insulator has served as a starting point for the search for other topological insulators [3].

SOC magnets with no charge degrees of freedom can also exhibit various Hall effects [4–13]. By exploiting ubiquitous spin-heat interactions [14], thermal Hall effects, in which a longitudinal temperature gradient induces a transverse heat current, has been used to probe SOC in such insulating magnets. For ordered magnets, thermal Hall effects are often accounted for by topologically nontrivial band structures of magnons, a quanta of spin-wave excitations from the ground states. For example, Matsumoto and Murakami [7] showed that thin-film ferromagnets have chiral edge states of magnetostatic spin-waves (that are associated with topologically nontrivial bulk band structures) and thus exhibit a thermal Hall effect. For magnets that are disordered by either thermal or quantum fluctuations, thermal Hall effects have been predicted by using the Schwinger boson or fermion representation of spins [15] that do not need a putative symmetry-breaking underlying state [5, 13].

In this Letter, we propose a simple spin Hamiltonian for SOC ferromagnets on the honeycomb lattice, which, as we shall show, exhibits a thermal-analog of spin Hall effects that are referred to as spin Nernst effects, in which a longitudinal temperature gradient generates a transverse spin current [14]. In the ordered phase, we show that the effective Hamiltonian for magnons is equivalent to the Haldane model [16], from which the topological property of the magnon bands can be inferred. We take an alternative Schwinger-boson (or bosonic spinon) rep-

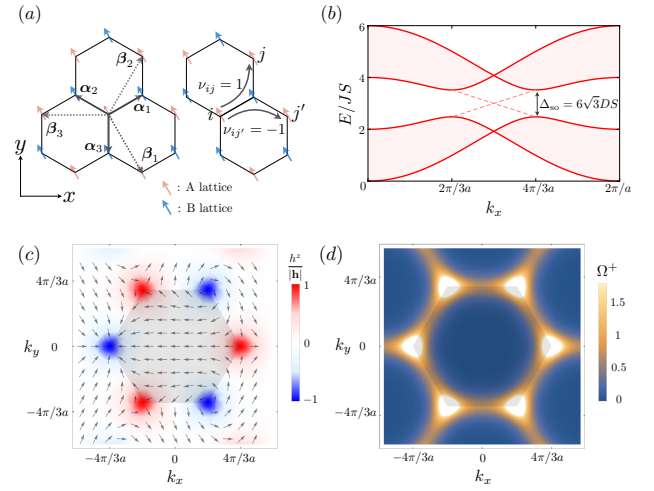


FIG. 1. (color online) (a) The honeycomb lattice structure and the relative sign  $\nu_{ij}$  of the DM interaction. (b) One-dimensional projection of the magnon bands [Eq. (4)], where the edge state is depicted as the dashed line. (c) The direction of  $\mathbf{h}(\mathbf{k})$  [Eq. (5)]. (d) The Berry curvature of the upper band,  $\Omega^+$ . For (b)-(d), the parameters  $D = 0.1J$  and  $B = 0$  are used. For (c)-(d), the shaded honeycomb is the first Brillouin zone. See the main text for detailed discussions.

resentation of spins to compute the spin Nernst conductivity at finite temperatures, where the magnon picture that is built on the well-ordered ground state may not be justified. We show that the mean-field spinon bands are topologically nontrivial and possess edge states owing to the equivalence to the Kane-Mele model. Lastly we propose a feasible way to realize the proposed Hamiltonian.

*Model.*—We consider a ferromagnetic material with SOC whose localized spins are arranged on a honeycomb lattice. The corresponding model Hamiltonian reads

$$H = -J \sum_{\langle i,j \rangle} \mathbf{S}_i \cdot \mathbf{S}_j - K \sum_{\langle i,j \rangle} S_i^z S_j^z + D \sum_{\langle\langle i,j \rangle\rangle} \nu_{ij} \hat{\mathbf{z}} \cdot (\mathbf{S}_i \times \mathbf{S}_j), \quad (1)$$

where the first and second terms represent the isotropic Heisenberg interaction ( $J > 0$ ) and the Ising interaction between nearest neighbors, respectively. The third term is the Dzyaloshinskii-Moriya (DM) interaction [17] between next-nearest neighbors, where the constants  $\nu_{ij} = -\nu_{ji} = \pm 1$  characterize the dependence of the interaction on the relative position of any two next-nearest spins, see Fig. 1(a). Notice that Eq. (1) represents the minimal effective Hamiltonian describing the above interactions invariant under the  $D_{6h}$  point-group symmetry of the lattice. For the particular experimental realization that we propose in this Letter (see below), the Ising contribution in  $H$  (1) can be safely neglected in what follows compared to the other terms. As we are interested in the topological properties of the model for both ordered and disordered phases, we introduce an external magnetic field applied along the  $z$  direction [and therefore a Zeeman coupling term  $-B \sum_i S_i^z$  in Eq. (1)] to stabilize the ferromagnetic ground state. For concrete discussions, we denote by  $d$  and by  $a = \sqrt{3}d$  the distance between nearest neighbors and next-nearest neighbors, respectively.

*Magnon picture.*—The system is ferromagnetically ordered at zero temperature and the uniform state  $\mathbf{S}_i \equiv S\hat{\mathbf{z}}$  represents the (classical) ground state of the model Hamiltonian (1) for  $B \geq 0$ . Application of the Holstein-Primakoff transformation  $S_i^\pm = S_i^x \pm iS_i^y = \left\{ \begin{array}{c} c_i \\ c_i^\dagger \end{array} \right\} (2S - n_i)^{1/2}$  and  $S_i^z = S - n_i$  with  $n_i = c_i^\dagger c_i$  yields the following effective magnon Hamiltonian

$$H_m = (3JS + B) \sum_i c_i^\dagger c_i - JS \sum_{\langle i,j \rangle} [c_i^\dagger c_j + \text{h.c.}] \quad (2)$$

$$- DS \sum_{\langle\langle i,j \rangle\rangle} [i\nu_{ij} c_i^\dagger c_j + \text{h.c.}],$$

where the expansion has been performed up to second order in the magnon operators  $\{c_i, c_i^\dagger\}$ . In such an approximation, the Hamiltonian reduces to the Haldane model [16].

The topological features of the magnon bands can be readily captured in the momentum representation: let  $\Psi_{\mathbf{k}} = (a_{\mathbf{k}}, b_{\mathbf{k}})$  be the spinor operators in the Fourier space, where  $a$  and  $b$  represent magnon annihilation operators on the sublattices  $\mathcal{A}$  and  $\mathcal{B}$ , respectively. Fourier transform of the Hamiltonian (2) then reads

$$H_m = \sum_{\mathbf{k} \in \text{B.Z.}} \Psi_{\mathbf{k}}^\dagger [(3JS + B)I + \mathbf{h}(\mathbf{k}) \cdot \boldsymbol{\tau}] \Psi_{\mathbf{k}}, \quad (3)$$

where  $\boldsymbol{\tau}$  is a pseudovector of Pauli matrices and the vector function  $\mathbf{h}(\mathbf{k})$  is defined in Eq. (5). The momentum dependence of the upper and lower energy bands becomes

$$E_m^\pm(\mathbf{k}) = 3JS + B \pm |\mathbf{h}(\mathbf{k})|, \quad (4)$$

so that in the absence of SOC ( $D = 0$ ) the upper and lower bands meet at two points,  $\mathbf{K} = (\frac{4\pi}{3a}, 0)$  and

$\mathbf{K}' = (\frac{2\pi}{3a}, \frac{2\pi}{\sqrt{3}a})$ , forming linearly-dispersed bands [18]. SOC opens an energy gap with opposite sign at these two points, making the band structure topologically nontrivial [2],

$$\mathbf{h}(\mathbf{k}) = \sum_j \begin{pmatrix} -JS \cos[\mathbf{k} \cdot \boldsymbol{\alpha}_j] \\ JS \sin[\mathbf{k} \cdot \boldsymbol{\alpha}_j] \\ 2DS \sin[\mathbf{k} \cdot \boldsymbol{\beta}_j] \end{pmatrix} = \begin{cases} 3\sqrt{3}DS\hat{\mathbf{z}} & \mathbf{k} = \mathbf{K} \\ -3\sqrt{3}DS\hat{\mathbf{z}} & \mathbf{k} = \mathbf{K}' \end{cases}, \quad (5)$$

where  $\{\alpha_i, \beta_i\}$  are defined in Fig. 1(a). The gap size between the upper and lower band is  $\Delta_{\text{so}} = 6\sqrt{3}DS$ . Figure 1(b) and (c) show the one-dimensional projection of the magnon bands  $E^\pm(\mathbf{k})$  and the direction of  $\mathbf{h}(\mathbf{k})$ , respectively, for the values  $D = 0.1J$ ,  $B = 0$  [19].

The Berry curvature of the upper and lower magnon bands can be calculated according to the formula  $\Omega_m^\pm = \mp \hat{\mathbf{n}} \cdot (\partial_{k_x} \hat{\mathbf{n}} \times \partial_{k_y} \hat{\mathbf{n}})/2$ , where  $\hat{\mathbf{n}}$  is the unit vector along  $\mathbf{h}$  [20]. Figure 1(d) plots the Berry curvature of the upper band. Notice that the Berry curvature is large around the corners of the Brillouin zone,  $\mathbf{K}$  and  $\mathbf{K}'$ , where the vector  $\mathbf{n}$  exhibits nontrivial topological textures that wrap a half of the unit sphere. The Chern numbers of the bands are evaluated as  $C^\pm = (1/2\pi) \int_{\text{B.Z.}} \Omega_m^\pm d^2k = \pm 1$ .

*Spinon picture.*—The magnon picture is built upon a magnetically-ordered ground state, and thus fails when the system is disordered by thermal or quantum fluctuations. Furthermore, the free magnon picture is not suitable for systems with small spins,  $S \sim 1$ , where magnon-magnon interactions play a crucial role. The Schwinger-boson representation of spins [15] provides an alternative approach to study the topological features of the energy bands in the above cases. The corresponding transformation reads  $S_i^+ = c_{i,\uparrow}^\dagger c_{i,\downarrow}$ ,  $S_i^- = c_{i,\downarrow}^\dagger c_{i,\uparrow}$  and  $S_i^z = (c_{i,\uparrow}^\dagger c_{i,\uparrow} - c_{i,\downarrow}^\dagger c_{i,\downarrow})/2$ . Here  $c_{i,s}$  ( $c_{i,s}^\dagger$ ) represents the annihilation (creation) operator of spin- $s$  bosons at the site  $i$ , which are referred to as Schwinger bosons or (bosonic) spinons. The local number constraint,  $\sum_s c_{i,s}^\dagger c_{i,s} = 2S$ , needs to be imposed to fulfill the spin- $S$  algebra. The Hamiltonian (1) in the spinon picture reads

$$H_s = -2J \sum_{\langle i,j \rangle} \chi_{ij}^\dagger \chi_{ij} + \frac{B}{2} \sum_i (c_{i,\uparrow}^\dagger c_{i,\uparrow} - c_{i,\downarrow}^\dagger c_{i,\downarrow}) \quad (6)$$

$$- \frac{D}{2} \sum_{\langle\langle i,j \rangle\rangle} i\nu_{ij} (\chi_{i,\uparrow}^\dagger \chi_{i,j,\downarrow} - \chi_{i,\downarrow}^\dagger \chi_{i,j,\uparrow})$$

$$+ \sum_i \lambda_i (c_{i,\uparrow}^\dagger c_{i,\uparrow} + c_{i,\downarrow}^\dagger c_{i,\downarrow} - 2S)$$

up to a constant, where  $\chi_{ij,s} = c_{i,s}^\dagger c_{j,s}$  are operators defined for pairs of sites for each spin  $s$ ,  $\chi_{ij} = (\chi_{i,\uparrow} + \chi_{i,\downarrow})/2$  and  $\lambda_i$  are the Lagrange multipliers related to the holonomic constraints. As the first and third terms are quartic in the spinon operators, the mean-field approach is well suited to study the energy bands of the Hamiltonian: assuming translational invariance,

we make the substitutions  $\chi_{ij}^\dagger \chi_{ij} \mapsto \eta^* \chi_{ij} + \eta \chi_{ij}^\dagger - |\eta|^2$ ,  $\chi_{ij,s}^\dagger \chi_{ij,-s} \mapsto \eta_s^* \chi_{ij,-s} + \eta_{-s} \chi_{ij,s}^\dagger - \eta_s^* \eta_{-s}$  and  $\lambda_i \mapsto \lambda$ , where  $\eta_{(s)}$  represents the expectation value  $\langle \chi_{ij,(s)} \rangle$  over (next-)nearest-neighbor pairs  $(i,j)$  and  $\lambda$  is the global Lagrange multiplier. We can always absorb the complex phase of  $\eta$  into the spinon operators, so that we will take  $\eta$  real in what follows. The identity  $\chi_{ij,s} = \chi_{ji,s}^\dagger$  leads to the expression  $\eta_s = \zeta_s + i\nu_{ij}\xi_s$  for the next-nearest-neighbor averages, with  $\zeta_s, \xi_s$  being real numbers. Thus, the mean-field Hamiltonian for the spinons becomes

$$\begin{aligned} H_s = & -\eta J \sum_{\langle i,j \rangle, s} [c_{i,s}^\dagger c_{j,s} + \text{h.c.}] \\ & + \frac{D}{2} \sum_{\langle\langle i,j \rangle\rangle, s} [i\nu_{ij} s \zeta_{-s} c_{i,s}^\dagger c_{j,s} + \text{h.c.}] \\ & + \frac{D}{2} \sum_{\langle\langle i,j \rangle\rangle, s} [s \xi_{-s} c_{i,s}^\dagger c_{j,s} + \text{h.c.}] \\ & + \sum_{i,s} \left( \lambda + s \frac{B}{2} \right) c_{i,s}^\dagger c_{i,s}. \end{aligned} \quad (7)$$

The mean fields  $\eta$  and  $\zeta_s$  represent short-ranged spin correlations [21], which must be finite for all temperatures. The first two terms in the above Hamiltonian then correspond to the Kane-Mele model [2], from which we can infer the nontrivial topology of the spinon-band structure and the existence of edge states for both spin-up and spin-down spinons. As we shall discuss below, the third term of Eq. (7) does not affect the topological features of the spinon bands. The spinon Hamiltonian in the momentum representation reads

$$H_s = \sum_{\mathbf{k} \in \text{B.Z.}, s} \Psi_{\mathbf{k},s}^\dagger [g_s(\mathbf{k})I + \mathbf{h}_s(\mathbf{k}) \cdot \boldsymbol{\tau}] \Psi_{\mathbf{k},s}, \quad (8)$$

where  $\Psi_{\mathbf{k},s} = (a_{\mathbf{k},s}, b_{\mathbf{k},s})$  is the spinor of annihilation operators,  $g_s(\mathbf{k}) = \lambda + s \frac{B}{2} + sD\xi_{-s} \sum_j \cos(\mathbf{k} \cdot \boldsymbol{\beta}_j)$ , and

$$\mathbf{h}_s(\mathbf{k}) = \sum_j \begin{pmatrix} -J\eta \cos[\mathbf{k} \cdot \boldsymbol{\alpha}_j] \\ J\eta \sin[\mathbf{k} \cdot \boldsymbol{\alpha}_j] \\ -Ds\zeta_{-s} \sin[\mathbf{k} \cdot \boldsymbol{\beta}_j] \end{pmatrix}. \quad (9)$$

The corresponding upper and lower energy bands for each spin  $s$  are then given by

$$E_s^\pm(\mathbf{k}) = g_s(\mathbf{k}) \pm |\mathbf{h}_s(\mathbf{k})|. \quad (10)$$

Notice that due to the similarity between the momentum dependence of  $\mathbf{h}_s(\mathbf{k})$  and  $\mathbf{h}(\mathbf{k})$  [Eq. (5)], we can conclude that for positive mean fields  $\eta$  and  $\zeta_\uparrow$  the bands corresponding to the spin-down spinons share the same topological features with the bands of magnons.

Self-consistency of the mean-field approach is guaran-

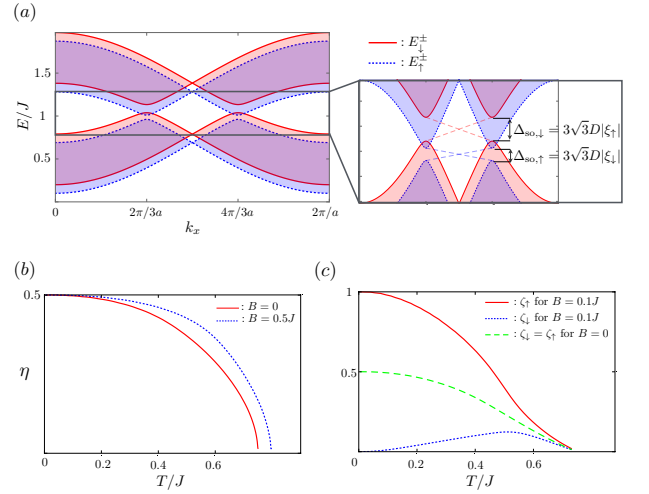


FIG. 2. (color online) (a) One-dimensional projection of the spinon bands [Eq. (10)] at the temperature  $T = 0.6J$  for the parameters  $S = 1/2, D = 0.1J, B = 0.1J$ . A zoom of the middle sector is shown in the inset, where the edge states are represented by the dashed lines. (b), (c) The dependence of the mean fields  $\eta, \zeta_\uparrow$ , and  $\zeta_\downarrow$  on the temperature for the parameters  $S = 1/2$  and  $D = 0.1J$ . Phase transitions of the mean fields at finite temperatures are artifacts of the mean-field approach. See the main text for detailed discussions.

teed through the equations in momentum space [22]

$$\begin{aligned} 2S &= \frac{1}{N} \sum_{\mathbf{k}, s} [\rho_s^-(\mathbf{k}) + \rho_s^+(\mathbf{k})], \quad (11) \\ 6N &= J \sum_{\mathbf{k}, s} \frac{\rho_s^-(\mathbf{k}) - \rho_s^+(\mathbf{k})}{|h_s(\mathbf{k})|} \left| \sum_i e^{i\mathbf{k} \cdot \boldsymbol{\alpha}_i} \right|^2, \\ \zeta_s &= \frac{1}{6N} \sum_{\mathbf{k}, s} [\rho_s^-(\mathbf{k}) + \rho_s^+(\mathbf{k})] \left[ \sum_i \cos(\mathbf{k} \cdot \boldsymbol{\alpha}_i) \right], \\ \xi_s &= -\frac{sD\zeta_{-s}}{6N} \sum_{\mathbf{k}, s} \frac{\rho_s^-(\mathbf{k}) - \rho_s^+(\mathbf{k})}{|h_s(\mathbf{k})|} \left| \sum_i \sin(\mathbf{k} \cdot \boldsymbol{\alpha}_i) \right|^2, \end{aligned}$$

where  $\rho_s^\tau(\mathbf{k}) = [\exp(E_s^\tau(\mathbf{k})/T) - 1]^{-1}$  is the Bose-Einstein distribution of spin- $s$  spinons in the  $\tau$  band and  $N$  is the number of unit cells. Note that the total number of spinons is fixed by the first condition. This enables the Bose condensation of spinons in the limit of zero temperature, which corresponds to magnetic ordering [21]. The mean-field spinon bands are obtained by solving self-consistently Eqs. (10) and (11), which are shown in Fig. 2(a) at the temperature  $T = 0.6J$  for the values  $S = 1/2, D = 0.1J, B = 0.1J$  of the physical constants. The SOC induces an energy gap  $\Delta_{\text{so},s} = 3\sqrt{3}D|\xi_{-s}|$  between the spin- $s$  spinon bands, whose Chern numbers read  $C_s^\pm = \mp s$ . Therefore, the topological nontriviality of the bulk bands for each spin supports the edge states drawn by the dashed line in the inset of Fig. 2(a). The thermal dependence of the mean fields  $\eta, \zeta_\uparrow$  and  $\zeta_\downarrow$  for the parameters  $S = 1/2, D = 0.1J$  is shown in Figs. 2(b)

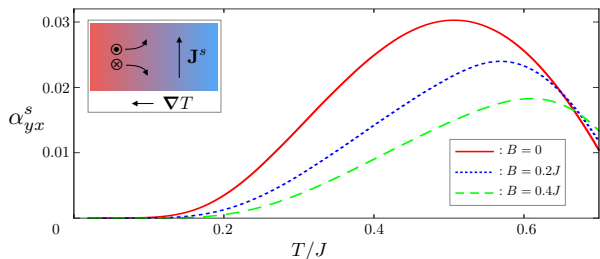


FIG. 3. (color online) The spin Nernst conductivity  $\alpha_{yx}^s$  as a function of temperature. The inset schematically shows a setup of an experiment and motions of spinons therein.

and (c). The vanishing of these fields at a finite temperature is unphysical because they represent short-ranged correlations between nearest- or next-nearest neighbors, and therefore must be finite for all temperatures. This phase transition is an artifact of mean-field treatments [23], which disappears when we account for fluctuations from the mean fields.

A connection of the spinon picture to the magnon picture can be established by taking the zero-temperature limit  $T \rightarrow 0$ . In the presence of an external magnetic field  $B > 0$ , the system becomes completely polarized along the  $z$  axis,  $\mathbf{S}_i \equiv S\hat{z}$ , as  $T \rightarrow 0$ . This polarization corresponds in the spinon picture to the Bose-Einstein condensation of spinons into the lowest-energy mode localized at the  $\mathbf{k} = 0$  state for the spin-up spinon band. The mean fields associated with this polarized state are  $\eta = S$ ,  $\zeta_{\uparrow} = 2S$ ,  $\zeta_{\downarrow} = \xi_{\uparrow} = \xi_{\downarrow} = 0$  and  $\lambda = 3JS + B/2$ , for which the spin-down spinon bands are equal to the magnon bands. The equivalence  $E_m^{\pm}(\mathbf{k}) \equiv E_{\downarrow}^{\pm}(\mathbf{k})$  provides the connection between two pictures.

*Spin Nernst effect.*—Spin-up and spin-down spinons experience opposite Berry curvatures,  $\Omega_{\uparrow}^{\pm}(\mathbf{k}) \equiv -\Omega_{\downarrow}^{\pm}(\mathbf{k})$ , in the absence of an external magnetic field. This can induce the spin Nernst effect [14], in which a transverse spin current is generated by applying a longitudinal temperature gradient,  $J_y^s = -\alpha_{yx}^s \partial_x T$ . The spinon picture is well suited to compute the spin Nernst conductivity  $\alpha_{yx}^s$  due to its applicability over a broad range of temperatures. We use the expression for  $\alpha_{yx}^s$  derived in Ref. [24] for the free magnon bands,  $\alpha_{yx}^s = -V^{-1} \sum_{\mathbf{k}, s, \tau} c_1[\rho_s^{\tau}(\mathbf{k})] \Omega_s^{\tau}(\mathbf{k})$ , where  $V = 3\sqrt{3}Nd^2/2$  is the volume of the system and  $c_1(x) = (1+x)\ln(1+x) - x\ln x$ .

Figure 3 shows the thermal dependence of the spin Nernst conductivity  $\alpha_{yx}^s$  for the physical parameters  $S = 1/2$ ,  $D = 0.1J$ . At zero temperature  $\alpha_{yx}^s = 0$  due to the absence of thermal excitations. As the temperature increases, spinons are thermally populated and  $\alpha_{yx}^s$  becomes finite. As the temperature approaches the ferromagnetic-exchange strength  $J$ , the magnitudes of the mean fields (that represent short-ranged correlations of spins) start decreasing, which eventually results in the

suppression of  $\alpha_{yx}^s$ . Application of a finite magnetic field increases the energies of the spin-down spinons, which in turn decreases the magnitude of the spin Nernst effect.

*Experimental realization.*—Although, to the best of our knowledge, the proposed Hamiltonian does not correspond to any existing material, the model may be engineered by depositing magnetic impurities on metals with strong spin-orbit coupling. Magnetic interactions are then mediated by itinerant electrons on the surface of the metal. The minimal Hamiltonian consists of two terms,  $\mathcal{H} = \mathcal{H}_{it} + \mathcal{J}\mathbf{S}_i \cdot \mathbf{s}(\mathbf{R}_i)$ . The first one describes the dynamics of electrons in the surface of the metal, whereas the second term describes the coupling between the localized spins  $\mathbf{S}_i$  and the spin density  $\mathbf{s}$  of itinerant electrons evaluated at the position of the impurities  $\mathbf{R}_i$ . For the former we can write

$$\mathcal{H}_{it} = \frac{\mathbf{p}^2}{2m_*} + V(\mathbf{r}) + \frac{\hbar}{2m_*^2 c^2} \mathbf{s} \cdot (\nabla V(\mathbf{r}) \times \mathbf{p}), \quad (12)$$

where  $\mathbf{p}$  is the momentum operator for itinerant electrons,  $m_*$  is their effective mass, and  $V(\mathbf{r})$  is the potential created by the impurities. The last term accounts for the spin-orbit interaction.

The potential  $V(\mathbf{r})$  admits a decomposition as a sum of harmonics of the honeycomb lattice since it must reflect the translational symmetry of the system when the impurities are arranged in a periodic lattice. For the sake of simplicity, we restrict the discussion to the 6 first harmonics,  $V(\mathbf{r}) = V \sum_{i=1..6} e^{i\mathbf{G}_i \cdot \mathbf{r}}$ . The original parabolic band is folded onto the Brillouin zone of the super-cell defined by the magnetic impurities, forming Dirac points at its corners. When the Fermi level of the metal approaches the Dirac points, the effective Hamiltonian describing the magnetic interactions reduces to Eq. (1), where

$$J \sim \frac{\epsilon_F \mathcal{J}^2 m_*^2}{\hbar^4} \sin\left(\frac{3d^2 m_* \epsilon_F}{\pi \hbar^2}\right), \quad (13)$$

$$D \sim -\frac{V \mathcal{J}^2}{2c^2 \hbar^2 d^2} \sin\left(\frac{3d^2 m_* \epsilon_F}{\pi \hbar^2}\right). \quad (14)$$

Here  $\epsilon_F$  is the Fermi level with respect to the Dirac points. The ratio between the characteristic wavelength of the electrons mediating the interaction and the distance between magnetic impurities controls the sign and the relative strength of the Heisenberg and DM couplings. Interestingly, with this approach the Ising-like term appears a second order effect in  $V$ , what justifies our previous assumption.

Another possibility would be to consider materials like chromium tri-halides, e.g.,  $\text{CrBr}_3$  or  $\text{CrCl}_3$ , which consist of weakly-coupled ferromagnetic honeycomb layers [25]. The interfacial DM interaction can be induced to those materials by the proximity effect with strong spin-orbit coupled materials, e.g., Pt or Ta, which may give rise to the physics described in the Letter.

*Discussion.*—We have proposed a simple spin Hamiltonian on the honeycomb lattice, whose properties can be

described by quasiparticles that behave like electrons in graphene and possess topologically nontrivial band structures.

In the spinon picture, we have neglected fluctuations of the Lagrangian multiplier  $\lambda_i$  and the bond operators  $\chi_{ij,s}$  from their mean-field values, which can be taken into account by, e.g., performing  $1/N$  corrections (the mean-field treatment corresponds to generalizing the spin symmetry group from  $SU(2)$  to  $SU(N)$  and taking  $N \rightarrow \infty$  limit) [26]. In particular, the phase fluctuations of the bond operators couple to the spinons as the  $U(1)$  gauge fields, which has been shown to result in confining the spinons in the ordered phases of some frustrated magnets, e.g., the Heisenberg antiferromagnet on the square lattice [27]. Investigating effects of the mean-field fluctuations in our spinon picture is a topic for future research.

After the completion of the manuscript, we became aware of a recent related work [28], in which the author studied the topological property of the magnon band on the honeycomb lattice and the associated thermal Hall effects. The spinon bands and spin Nernst effects, however, are not discussed in the reference.

We are grateful to Yong P. Chen and Fenner Harper for insightful discussions. This work was supported by the Army Research Office under Contract No. 911NF-14-1-0016, by the U.S. Department of Energy, Office of Basic Energy Sciences under Award No. DE-SC0012190, and by the NSF-funded MRSEC under Grant No. DMR-1420451. RZ thanks the Fundaci3n Ram3n Areces for the postdoctoral fellowship within the XXVII Convocatoria de Becas para Ampliaci3n de Estudios en el Extranjero en Ciencias de la Vida y de la Materia.

---

[1] J. Sinova, S. O. Valenzuela, J. Wunderlich, C. H. Back, and T. Jungwirth, *Rev. Mod. Phys.* **87**, 1213 (2015), and references therein.  
 [2] C. L. Kane and E. J. Mele, *Phys. Rev. Lett.* **95**, 226801 (2005).  
 [3] M. Z. Hasan and C. L. Kane, *Rev. Mod. Phys.* **82**, 3045 (2010), and references therein.  
 [4] S. Fujimoto, *Phys. Rev. Lett.* **103**, 047203 (2009).

[5] H. Katsura, N. Nagaosa, and P. A. Lee, *Phys. Rev. Lett.* **104**, 066403 (2010).  
 [6] F. D. M. Haldane and D. P. Arovas, *Phys. Rev. B* **52**, 4223 (1995).  
 [7] R. Matsumoto and S. Murakami, *Phys. Rev. Lett.* **106**, 197202 (2011); *Phys. Rev. B* **84**, 184406 (2011).  
 [8] L. Zhang, J. Ren, J.-S. Wang, and B. Li, *Phys. Rev. B* **87**, 144101 (2013).  
 [9] R. Shindou, J.-i. Ohe, R. Matsumoto, S. Murakami, and E. Saitoh, *Phys. Rev. B* **87**, 174402 (2013).  
 [10] R. Shindou, R. Matsumoto, S. Murakami, and J.-i. Ohe, *Phys. Rev. B* **87**, 174427 (2013).  
 [11] R. Matsumoto, R. Shindou, and S. Murakami, *Phys. Rev. B* **89**, 054420 (2014).  
 [12] A. Mook, J. Henk, and I. Mertig, *Phys. Rev. B* **89**, 134409 (2014).  
 [13] H. Lee, J. H. Han, and P. A. Lee, *Phys. Rev. B* **91**, 125413 (2015).  
 [14] G. E. W. Bauer, E. Saitoh, and B. J. van Wees, *Nat. Mater.* **11**, 391 (2012), and references therein.  
 [15] D. P. Arovas and A. Auerbach, *Phys. Rev. B* **38**, 316 (1988); A. Auerbach and D. P. Arovas, *Phys. Rev. Lett.* **61**, 617 (1988).  
 [16] F. D. M. Haldane, *Phys. Rev. Lett.* **61**, 1029 (1988).  
 [17] I. Dzyaloshinsky, *Journal of Physics and Chemistry of Solids* **4**, 241 (1958); T. Moriya, *Phys. Rev.* **120**, 91 (1960).  
 [18] J. Fransson, A. M. Black-Schaffer, and A. V. Balatsky, arXiv:1512.04902.  
 [19] To be precise, Fig. 1(b) is obtained by combining the plots of  $E^\pm(k_x, k_y)$  as a function of  $k_x$  for all  $k_y$ .  
 [20] D. Xiao, M.-C. Chang, and Q. Niu, *Rev. Mod. Phys.* **82**, 1959 (2010).  
 [21] S. Sarker, C. Jayaprakash, H. R. Krishnamurthy, and M. Ma, *Phys. Rev. B* **40**, 5028 (1989).  
 [22] Formally, the self-consistency conditions can be obtained by demanding the functional derivative with respect to the mean fields of the free energy  $H = H_s + 3JN|\eta|^2 - 3DN \sum_s s \zeta_s \xi_{-s} - 2SN\lambda$  to vanish.  
 [23] O. Tchernyshyov and S. L. Sondhi, *Nucl. Phys. B* **639**, 429 (2002).  
 [24] A. A. Kovalev and V. Zyuzin, arXiv:1509.05847.  
 [25] L. J. D. Jongh and A. R. Miedema, *Adv. Phys.* **50**, 947 (2001), and references therein.  
 [26] A. E. Trumper, L. O. Manuel, C. J. Gazza, and H. A. Ceccatto, *Phys. Rev. Lett.* **78**, 2216 (1997).  
 [27] N. Read and S. Sachdev, *Phys. Rev. Lett.* **66**, 1773 (1991); T. K. Ng, *Phys. Rev. B* **47**, 11575 (1993).  
 [28] S. A. Owerre, arXiv:1603.04331.